Supplement of Atmos. Chem. Phys., 26, 9967–9980, 2026
https://doi.org/10.5194/acp-26-9967-2026-supplement

Atmospheric Chemistry and Physics
Open Access

Supplement of

Characterizing efflorescence regimes in organic–inorganic aerosols using thermodynamically modeled viscosity

Shanshan Chen et al.

Correspondence to: Qishen Huang (qishenh@bit.edu.cn)

Table S1. List of training datasets used for the parameterization of ERH in organic-inorganic aerosol systems. The datasets include OIR (molar ratio of organic compounds to inorganic salts, excluding water), oxygen-to-carbon ratios calculated from OIR (O:C), x_{org}, $T_g(\omega_{org})$, ω_{org}, viscosity, the estimated sensitivity/uncertainty of the viscosity, and ERH. All viscosity values were computed using the AIOMFAC model. The following data are reported under room temperature conditions (298 ± 10 K). The relative humidity decreasing at a rate of less than 0.1% s^{-1}.

Compound	OIR	x_{org}	ω_{org}	O:C	$T_g(\omega_{org})$	ERH (%)	$\log_{10}(\eta$/[Pa.s])	$\pm\log_{10}(\eta$ sens./[Pa.s])	Reference
Glucose ($C_6H_{12}O_6$)/AS	0.25	0.2	0.19	1.00	146.09	37	-1.56	0.02	Chang(Chang, 2020)
	0.33	0.25	0.24	1.00	149.41	34.5	-1.31	0.03	
	0.50	0.33	0.33	1.00	155.49	31.5	-0.83	0.05	
Sucrose ($C_{12}H_{22}O_{11}$)/AS	0.25	0.2	0.32	0.92	169.80	32.3	-0.74	0.03	Xu et al.(Xu et al., 2022)
	0.50	0.33	0.50	0.92	197.97	24.4	0.80	0.18	
	0.25	0.2	0.33	0.92	171.79	25.4	-0.44	0.05	Wang et al.(Wang et al., 2017a)
	0.33	0.25	0.41	0.92	182.97	21.2	0.05	0.14	
	0.50	0.33	0.51	0.92	199.51	21.1	1.28	0.28	
Glycerol ($C_3H_8O_3$)/AS	0.25	0.2	0.10	1.00	137.87	51.20	-2.12	0.01	Xu et al.(Xu et al., 2022)
	0.50	0.33	0.18	1.00	139.56	49.50	-2.00	0.01	
	1.00	0.5	0.30	1.00	142.61	45.60	-1.77	0.02	
	2.00	0.67	0.50	1.00	149.00	29.70	-1.03	0.05	
	3.00	0.75	0.61	1.00	153.53	22.80	-0.67	0.08	
	0.14	0.13	0.09	1.00	137.81	30.5	-1.78	0.02	Cai et al.(Cai et al., 2017)
	0.5	0.33	0.19	1.00	139.83	41.00	-1.85	0.01	
	0.33	0.25	0.13	1.00	138.64	42.00	-1.94	0.01	
	0.25	0.2	0.10	1.00	138.02	43.00	-1.98	0.01	
	0.25	0.2	0.18	1.33	141.65	36.70	-1.09	0.04	Xu et al.(Xu et al., 2022)
	0.50	0.33	0.25	1.33	144.32	26.50	-0.38	0.09	
	1.00	0.5	0.41	1.33	151.11	21.50	0.34	0.19	
	2.00	0.67	0.55	1.33	159.03	28.7	0.23	0.15	
Malonic acid $C_3H_4O_4$/AS	0.4286	0.3	0.23	1.33	143.45	22.6	-0.25	0.11	Braban et al.(Braban and Abbatt, 2004)
	0.1428	0.125	0.09	1.33	138.60	28	-0.99	0.05	
	0.0833	0.077	0.05	1.33	137.50	31	-1.27	0.04	
	0.6	0.375	0.17	1.33	141.41	24.3	-0.51	0.08	Parsons et al.(Parsons et al., 2004)
	0.33	0.25	0.18	1.33	141.64	30.3	-0.74	0.06	
Citric acid $C_6H_8O_7$/AS	0.25	0.25	0.21	1.17	148.97	37.30	-1.05	0.04	Xu et al[2].
	0.50	0.33	0.36	1.17	161.31	24.80	0.73	0.23	
	0.33	0.25	0.29	1.17	155.60	23	0.19	0.18	Shi et al.(Shi et al., 2017)

1,2,6-Hexanetriol $C_6H_{14}O_3$/AS	1.00	0.5	0.37	0.50	146.84	47.45	-1.70	0.02	Ma et al.(Ma et al., 2021)
	0.25	0.2	0.13	0.50	139.31	46.4	-2.07	0.01	
	2.00	0.67	0.56	0.50	154.76	43.2	-1.07	0.05	
Oxalic acid $C_2H_2O_4$/AS	1.00	0.50	0.34	2.00	148.31	44.3	-2.53	0.07	Wang et al.(Wang et al., 2017b)
	3.00	0.75	0.45	2.00	154.08	64.4	-2.79	0.02	
	0.33	0.25	0.17	2.00	141.42	34.4	-2.25	0.13	
Glutaric acid $C_5H_8O_4$/AS	1.5	0.6	0.24	0.80	144.07	22	0.34	0.24	Pant et al.(Pant et al., 2004)
	0.1111	0.1	0.02	0.80	136.65	32	-1.50	0.02	
	1.00	0.50	0.07	0.80	137.96	36.5	-0.81	0.07	Wu(Wu, 2017)
DEMA/AS Diethyl malonic acid	2.00	0.67	0.63	0.57	167.99	43.06	-0.20	0.13	
DMSA/AS 2,2-Dimethyl succinic acid	2.00	0.67	0.60	0.67	164.55	42.04	-0.39	0.11	
DMGA/AS 3,3-Dimethyl glutaric acid	2.00	0.6	0.63	0.57	167.99	43.49	-0.20	0.13	Huang et al.(Huang et al., 2024)
HMMA/AS DL-4-Hydroxy-3-methoxymandelic acid	2.00	0.67	0.65	0.56	180.87	38.74	-0.13	0.11	
Oxalic acid/KCl $C_2H_2O_4$	0.33	0.25	0.12	2.00	139.90	73	-2.59	0.00	
	1	0.5	0.27	2.00	145.59	72	-2.23	0.01	
	3	0.75	0.40	2.00	151.47	75	-1.97	0.00	
Malonic acid/KCl $C_3H_4O_4$	0.33	0.25	0.19	1.33	141.20	53	-2.27	0.01	Wang(Wang, 2018)
	1	0.5	0.03	1.33	153.00	42	-1.48	0.03	
Maleic acid/KCl $C_4H_4O_4$	0.33	0.25	0.22	1.00	143.36	44	-2.13	0.01	
	1	0.5	0.51	1.00	156.45	33	-1.13	0.06	
	3	0.75	0.72	1.00	172.18	33	-1.90	0.12	
Glutaric acid/NaCl $C_5H_8O_4$	0.33	0.25	0.18	0.80	141.95	66	-2.34	0.00	Ghorai et al.(Ghorai et al., 2014)
	1	0.5	0.01	0.80	152.97	59	-1.89	0.01	
	0.25	0.2	0.20	0.80	142.41	45	-2.07	0.01	Pant et al.(Pant et al., 2004)
	1.5	0.6	0.64	0.80	165.94	39	-0.85	0.07	
	2.33	0.7	0.75	0.80	175.63	31	0.02	0.16	
Malonic acid /NaCl $C_3H_4O_4$	0.33	0.25	0.56	1.33	141.20	62	-2.22	0.00	Ghorai et al.(Ghorai et al., 2014)
	0.50	0.33	0.63	1.33	146.81	36.2	-1.48	0.02	Laskina et

									al.(Laskina et al., 2015)
	1.00	0.5	0.43	1.00	146.49	32	-0.66	0.08	Yu et al.(Yu et al., 2012)
	0.50	0.33	0.27	1.00	141.84	35.7	-1.07	0.05	
Glycerol	0.125	0.11	0.07	1.00	137.37	57	-2.03	0.01	
/$NaNO_3$	0.25	0.2	0.14	1.00	138.77	51	-1.76	0.02	
($C_3H_8O_3$)	0.5	0.33	0.52	1.00	141.15	47	-1.57	0.03	Ren et al.(Ren et al., 2016)
	1	0.5	0.42	1.00	146.19	35	-0.86	0.06	
	2	0.67	0.64	1.00	154.92	15	0.35	0.26	
Sucrose/	0.25	0.2	0.45	0.92	189.01	20.7	1.95	0.07	
$NaNO_3$ ($C_{12}H_{22}O_{11}$)	0.125	0.11	0.28	0.92	164.79	25.4	0.27	0.05	Ji et al.(Ji et al., 2017)

Table S2. The validation dataset for predicting ERH in mixed aerosol systems consists of 12 organic compounds and 4 inorganic salts. The following data are calculated at room temperature condition 298 K.

[a] calculated using the AIOMFAC model

[b] experimentally measured

Compound	OIR	ERH(%)	$\log_{10}(\eta/[Pa.s])$	Reference
HXT/AS/SUS	1:1:0	46	-1.70 [a]	Ye et al.(Ye et al., 2025)
	1:1:0.1	46.8	-1.53 [a]	
	1:1:0.25	41	-0.98 [a]	
	1:1:0.5	25	0.78 [a]	
	1:1:0.75	25	1.43 [a]	
HXT/AS/GLY	1:1:0	45	-1.68 [a]	
	1:1:0.1	46	-1.66 [a]	
	1:1:0.25	48	-1.67 [a]	
	1:1:0.5	48	-1.58 [a]	
	1:1:0.75	46	-1.46 [a]	
	1:1:1	42	-1.27 [a]	
HXT/AS/CA	1:1:0	45	-1.68 [a]	
	1:1:0.1	40	-1.25 [a]	
	1:1:0.25	37.5	-0.73 [a]	
	1:1:0.5	35	-0.019 [a]	
	1:1:0.75	35	0.45 [a]	
HMMA/AS	0.34	40.3	-1.57 [a]	Bertram et al.(Bertram et al., 2011)
	0.92	39.8	-0.99 [a]	
	2.06	37.8	-0.057 [a]	
DHBA/AS	0.21	33.6	-0.76 [a]	
	0.39	36.7	-0.82 [a]	
	0.63	34.2	-0.84 [a]	
	0.95	32.9	-0.83 [a]	
DMSA/AS	0.35	32.9	-1.35 [a]	
	0.61	33.9	-1.07 [a]	
	1.12	40.3	-0.82 [a]	
	1.38	32.1	-0.12 [a]	
Maleic acid/ $NaNO_3$	1：3	0	3.75 [a]	Chang(Chang, 2020)
	1：1	0	3.73 [a]	
	3：1	0	3.72 [a]	
Glutaric acid/NaCl	3：1	0	3.38 [a]	Pant et al.(Pant et al., 2004)
Malonic acid /KCl	3：1	0	3.51 [a]	Wang(Wang, 2018)
Raffinose/AS	1：1	0	6.00 [b]	Ushijima et al.(Ushijima et al., 2021)
Citric acid /AS	1：1	0	7.54 [b]	Sheldon et al.(S. Sheldon et al., 2023)
	2：1	0	7.54 [b]	
	3：1	0	7.70 [b]	

Table S3. Functional group decomposition of organic compounds in AIOMFAC.

Compound	Subgroup	Quantity
Sucrose ($C_{12}H_{22}O_{11}$)	CH_2_hydroxy	3
	CH_hydroxy	5
	OH	8
	CHO(ether)	3
	C	1
Glucose ($C_6H_{12}O_6$)	CH_2_hydroxy	1
	CH_hydroxy	4
	OH	5
	CHO(ether)	1
1,2,6-Hexanetriol ($C_6H_{14}O_3$)	CH_2[alc]	3
	CH	1
	CH_2	2
	OH	3
	C	1
DMSA 2,2-Dimethyl succinic acid	CH_3	2
	CH_2	1
	COOH	2
DMGA 3,3-Dimethyl glutaric acid	CH_3	2
	CH_2	2
	C	1
	COOH	2
DEMA Diethyl malonic acid	C	1
	CH_3	2
	CH_2	2
	COOH	2
DHBA 2,5-Dihydroxybenzoic acid	ACH	3
	AC	1
	ACOH	2
	COOH	1
HMMA DL-4-Hydroxy-3-methoxymandelic acid	ACH	3
	ACOH	1
	CH_3O	1
	CH-[OH]	1
	OH	1
	COOH	1

Table S4. Input parameters employed for the calculation of glass transition temperatures T_g using the model developed by Armeli et al.

Compound	FG Mode								Optional*	SMILES Mode
	-CH_3	-CH_2	-CH	-C-	-OH	-O-	=O	DBE	T_m / K	SMILES String
glucose	0	1	4	1	5	0	1	1	420	C(C1C(C(C(C(O1)O)O)O)O)O
sucrose	0	3	8	1	8	3	0	2	457	C(C1C(C(C(C(O1)OC2(C(C(C(O2)CO)O)O)CO)O)O)O)O
glycerol	0	2	1	0	3	0	0	0	291	OCC(O)CO
citric acid	0	2	0	4	4	0	3	3	432	C(C(=O)O)C(CC(=O)O)(C(=O)O)O
1,2,6-hexanetriol	0	5	1	0	3	0	0	0	300	C(CCO)CC(CO)O
Malonic acid	0	1	0	2	2	0	2	2	408	C(C(=O)O)C(=O)O
Oxalic acid	0	0	0	2	2	0	2	0	462.5	C(=O)(C(=O)O)O
Glutaric acid	0	3	0	2	2	0	2	2	371	C(CC(=O)O)CC(=O)O
Maleic acid	0	0	2	2	2	0	2	3	403.5	C(=C\C(=O)O)\C(=O)O
DEMA	2	2	0	3	2	0	2	2	395	CCC(CC)(C(=O)O)C(=O)O
DMSA	2	1	0	3	2	0	2	2	413.5	CC(C)(CC(=O)O)C(=O)O
DMGA	2	2	0	3	2	0	2	2	376.5	CC(C)(CC(=O)O)CC(=O)O
HMMA	1	0	4	4	3	1	1	5	405	COC1=C(C=CC(=C1)C(C(=O)O)O)O

* T_m is an optional input parameter for both modes

Table S5. T_g of pure organic compounds calculated using the method of Armeli et al.

Compound	T_g (FGM with T_m)	T_g (FGM no T_m)	T_g (SM with T_m)	T_g (SM no T_m)
Glucose ($C_6H_{12}O_6$)	295.8	300.2	275.3	282.3
Sucrose ($C_{12}H_{22}O_{11}$)	344	342.4	342.5	339.1
Glycerol ($C_3H_8O_3$)	187.4	187.5	187.4	187.7
Malonic acid $C_3H_4O_4$	258.9	231.3	259	234.9
Citric acid $C_6H_8O_7$	284.4	284.4	283.6	283.2
1,2,6-Hexanetriol $C_6H_{14}O_3$	202.3	201.5	203.6	202.7
Oxalic acid $C_2H_2O_4$	276	226.8	271.9	224.9
Glutaric acid $C_5H_8O_4$	261.9	242.4	250.1	252.5
DEMA Diethyl malonic acid	274.8	266.2	271.1	270.5
DMSA 2,2-Dimethyl succinic acid	282	262.5	277.9	269.5
DMGA 3,3-Dimethyl glutaric acid	267.5	266.2	265.6	261.5
HMMA DL-4-Hydroxy-3-methoxymandelic acid	276.1	296.2	276.1	284
Maleic acid $C_4H_4O_4$	264.1	242.6	261.6	251.8

Table S6. $T_g(\omega_{org})$ of the mixed aqueous systems derived via the Gordon–Taylor equation assuming a k_{GT} of 2.5 and using the T_g of the pure compound calculated from Armeli et al. using the model.

Compound	ω_{org}	$T_{g(\omega org)}$ (FGM with T_m)	$T_{g(\omega org)}$ (FGM no T_m)	$T_{g(\omega org)}$ (SM with T_m)	$T_{g(\omega org)}$ (SM no T_m)
Glucose ($C_6H_{12}O_6$)/AS	0.19	149.74	150.12	147.98	148.58
	0.24	154.27	154.88	152.04	152.84
	0.33	162.55	163.61	159.48	160.64
Sucrose ($C_{12}H_{22}O_{11}$)/AS	0.32	168.70	168.45	168.47	167.93
	0.50	195.96	195.50	195.53	194.55
	0.33	170.63	170.37	170.38	169.82
	0.41	181.45	181.10	181.12	180.38
	0.51	197.45	196.98	197.01	196.01
Glycerol ($C_3H_8O_3$)/AS	0.10	138.12	138.12	138.12	138.13
	0.18	140.03	140.04	140.03	140.06
	0.30	143.48	143.50	143.48	143.53
	0.50	150.73	150.76	150.73	150.81
	0.61	155.86	155.89	155.86	155.97
Malonic acid $C_3H_4O_4$/AS	0.09	138.05	138.06	138.05	138.06
	0.19	140.34	140.34	140.34	140.36
	0.13	138.99	138.99	138.99	139.00
	0.10	138.29	138.29	138.29	138.30
	0.18	145.86	143.65	145.87	143.94
	0.25	150.51	147.25	150.52	147.67
	0.41	162.36	156.44	162.38	157.21
	0.55	176.16	167.14	176.20	168.32
	0.23	149.00	146.08	149.01	146.46
	0.09	140.53	139.52	140.54	139.65
	0.05	138.61	138.03	138.62	138.10
Citric acid $C_6H_8O_7$/AS	0.17	145.43	143.31	145.43	143.59
	0.18	145.84	143.63	145.84	143.91
	0.21	149.89	149.89	149.82	149.78
	0.36	163.11	163.11	162.97	162.89
	0.29	157.00	157.00	156.88	156.83
1,2,6-Hexanetriol $C_6H_{14}O_3$/AS	0.37	148.78	148.62	149.03	148.86
	0.13	139.91	139.86	139.98	139.93
	0.56	158.11	157.84	158.54	158.24
Oxalic acid $C_2H_2O_4$/AS	0.34	159.55	151.28	158.86	150.96
	0.45	170.60	158.44	169.59	157.97
	0.17	146.36	142.72	146.06	142.58
Glutaric acid $C_5H_8O_4$/AS	0.24	150.04	147.86	148.72	148.99
	0.02	137.14	136.96	137.03	137.05

	0.07	139.41	138.88	139.09	139.16
DEMA/AS Diethyl malonic acid	0.63	191.78	188.32	190.29	190.05
DMSA/AS 2,2-Dimethyl succinic acid	0.60	191.16	183.79	189.61	186.44
DMGA/AS 3,3-Dimethyl glutaric acid	0.63	188.84	188.32	188.08	186.43
HMMA/AS DL-4-Hydroxy-3-methoxymandelic acid	0.65	195.10	203.58	195.10	198.44
Oxalic acid/KCl $C_2H_2O_4$	0.12	143.47	140.85	143.25	140.74
	0.27	154.35	147.90	153.81	147.65
	0.40	165.60	155.20	164.73	154.80
Malonic acid/KCl $C_3H_4O_4$	0.19	146.47	144.12	146.48	144.42
	0.03	137.31	137.02	137.31	137.05
Maleic acid/KCl $C_4H_4O_4$	0.22	149.26	147.04	149.00	147.99
	0.51	173.15	166.92	172.43	169.59
	0.72	201.50	190.51	200.22	195.21
Glutaric acid/NaCl $C_5H_8O_4$	0.18	146.34	144.74	145.37	145.57
	0.01	136.44	136.37	136.40	136.41
	0.20	147.14	145.42	146.10	146.31
	0.64	188.06	180.00	183.18	184.18
Malonic acid /NaCl $C_3H_4O_4$	0.75	204.92	194.24	198.46	199.77
	0.56	177.21	167.95	177.24	169.16
	0.63	186.36	175.05	186.40	176.52
Glycerol /$NaNO_3$ ($C_3H_8O_3$)	0.43	147.91	147.93	147.91	147.98
	0.27	142.62	142.63	142.62	142.65
	0.07	137.55	137.55	137.55	137.56
	0.14	139.11	139.12	139.11	139.13
	0.52	151.57	151.60	151.57	151.66
Sucrose/$NaNO_3$ ($C_{12}H_{22}O_{11}$)	0.42	147.54	147.56	147.54	147.60
	0.64	157.50	157.54	157.50	157.63
	0.45	187.29	314.83	183.84	186.08
	0.28	163.85	307.44	161.98	163.20

Table S7. Comparison of the experimentally measured T_g of organic compounds with values predicted using the method of Li et al. and the method of Armeli et al.

	T_g / K					
			$T_{g\,Armeli}$(Armeli et al., 2023)			
Compound	$T_{g\,literature}$(Armeli Iapichino et al., 2023)	$T_{g\,Li}$(Li et al., 2020)	FGM with T_m	FGM no T_m	SM with T_m	SM no T_m
Glucose	303	253.32	295.8	300.2	275.3	282.3
Sucrose	334	350.97	344.0	342.4	342.5	339.1
Glycerol	186	181.38	187.4	187.5	187.4	187.7
Citric acid	284.35	274.53	284.4	284.4	283.6	283.2
1,2,6-Hexanetriol	204.15	192.25	202.3	201.5	203.6	202.7
Mean Absolute Error / K		18.6	4.0.	3.1	7.8	6.0

Table S8. The equation obtained after linearly regressing various physicochemical parameters with ERH and the R^2.

Parameter	R^2	Fitting equation
O:C	0.09	y=26.58+11.1x
ω_{org}	0.06	y=44.00-17.042x
$T_g(\omega_{org})$	0.14	y=89.79-0.34x
Viscosity	0.65	y=27.40-10.23x

Table S9. Prediction model for ERH using multivariate function fitting with O:C, ω_{org}, and T_g as input variables.

Parameter	**R^2**	**Fitting equation**
O:C, $T_g(\omega_{org})$, ω_{org}	0.18	ERH=75.26+8.035 (O:C)-0.30($T_g(\omega_{org})$) -2.22(ω_{org})

	Value	Std. Error	t-value	Prob>t
Constant	75.26	20.99	3.586	0.001
"O:C"	8.035	4.397	1.828	0.072
" $T_g(\omega_{org})$"	-0.303	0.142	-2.136	0.037
"ω_{org}"	-2.217	10..848	0.204	0.839

Table S10. Comparison of multivariate ERH prediction models incorporating viscosity, O:C, ω_{org}, and T_g with the viscosity-ERH model.

Parameter	**R^2**	**Fitting equation**	**Sig F change**
Viscosity	0.65	y=-10.23(viscosity)+27.40	0.000
Viscosity, O:C, $T_g(\omega_{org})$, ω_{org}	0.69	y=-0.887(O:C)+0.246($T_g(\omega_{org})$) +0.516(ω_{org})-12.7(viscosity)-11.91	0.041

Parameter	Value	Std. Error	t-value	Prob>|t|
Constant	27.390	1.439	19.029	0.000
"Viscosity"	-10.230	0.946	-10.833	0.000
Constant	-11.908	15.654	-0.761	0.450
"O:C"	-0.887	2.867	-0.309	0.758
"Viscosity"	-12.70	1.268	-10.017	0.000
"$T_g(\omega_{org})$"	0.246	0.104	2.374	0.021
"ω_{org}"	0.516	6.727	0.077	0.939

Table S11. Comparison and parameter analysis of the multivariate ERH prediction model (using viscosity, O:C, ω_{org}, and T_g as input variables) versus the bivariate viscosity-T_g model.

Parameter	**R^2**	**Fitting equation**	**Sig F change**
Viscosity, $T_g(\omega_{org})$	0.691	y=0.251($T_g(\omega_{org})$)-12.579(Viscosity)-13.284	0.000
Viscosity, O:C, $T_g(\omega_{org})$, ω_{org}	0.695	y=3.569(O:C)+0.25 ($T_g(\omega_{org})$) – 2.621(ω_{org})-12.157(Viscosity)-13.428	0.949

Parameter	Value	Std. Error	t-value	Prob>|t|
Constant	-13.284	13.700	-0.970	0.336
"Viscosity"	-12.579	1.187	-10.598	0.000
"$T_g(\omega_{org})$"	0.251	0.084	2.984	0.004
Intercept	-11.908	15.654	-0.761	0.450
"O:C"	-0.887	2.867	-0.309	0.758
"Viscosity"	-12.70	1.268	-10.017	0.000
"$T_g(\omega_{org})$"	0.246	0.104	2.374	0.021
"ω_{org}"	-0.516	6.727	0.077	0.939

Table S12. Viscosity changes for representative fixed chemical systems across an RH of 20%-60%, including the slopes of the viscosity-RH relationships (ranging from approximately -10 to -60) and the correlation between viscosity at a fixed RH and ERH.

Compound	OIR	20	30	40	50	60	Fitting equation
Glutaric acid/NaCl	1:4	-1.54	-1.79	-1.99	-2.14	-2.31	y = -52.20x-62.11
Glycerol/$NaNO_3$	1:4	-0.28	-0.93	-1.33	-2.21	-2.38	y = -22.94x+11.17
Sucrose/$NaNO_3$	1:4	2.12	0.71	-0.066	-0.69	-1.18	y = -11.87x+42.15
Citric acid /AS	1:4	0.05	-0.7	-1.12	-1.48	-1.78	y = -21.69x+18.14

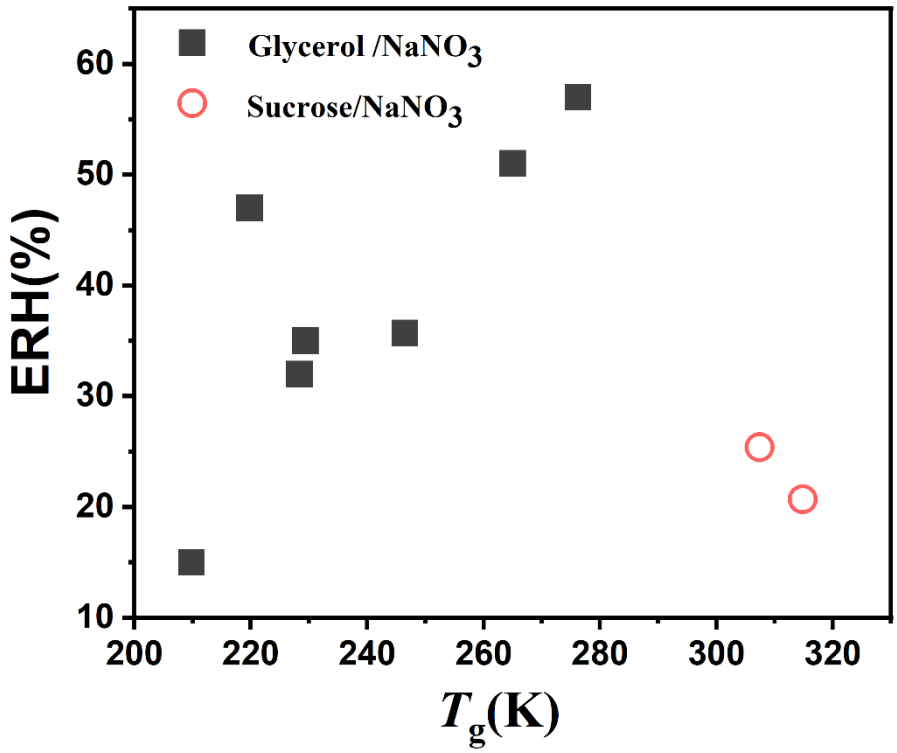

Figure S1. Calculated dry T_g of glycerol/$NaNO_3$ and sucrose/ $NaNO_3$ systems at various mixing ratios, plotted against their respective efflorescence points. The calculations are based on the reported T_g of 290 K for $NaNO_3$.

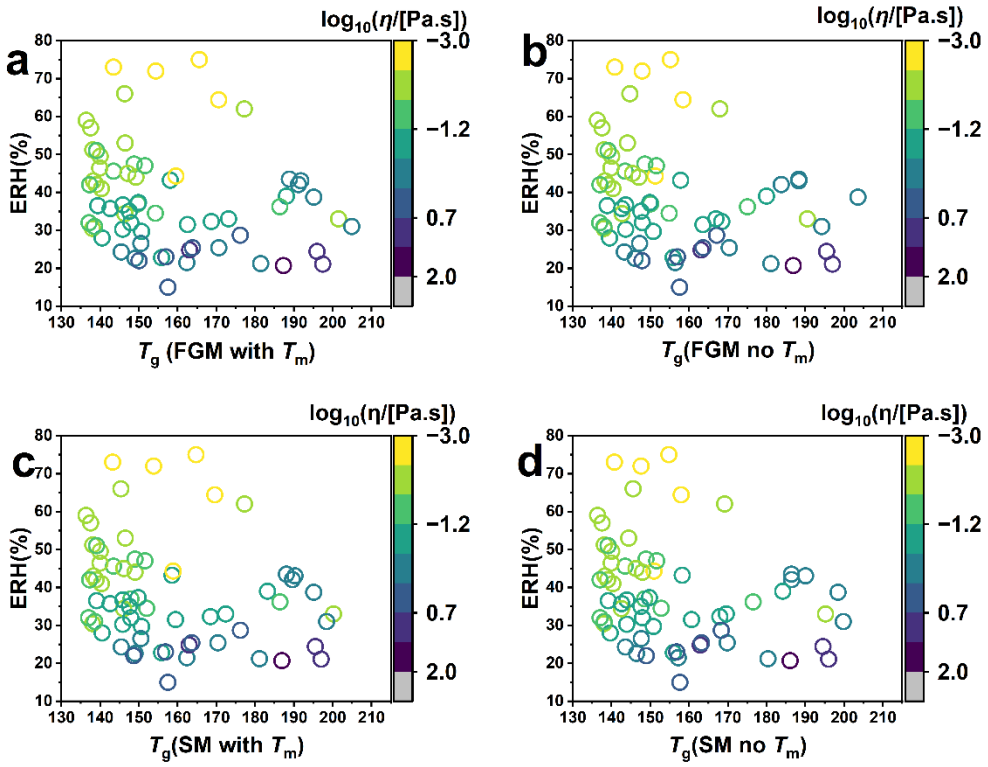

Figure S2. Relationships between the ERH of organic-inorganic mixed aerosols. (a) T_g(FGM with T_m), (b) T_g(FGM no T_m), (c) T_g(SM with T_m), and (d) T_g(SM no T_m), T_g of organic compounds calculated using the methodology and online predictor of Armeli et al. (Armeli et al., 2023), and the resulting T_g of organic-inorganic mixtures derived via the Gordon-Taylor equation. All empirical ERH values were measured within a temperature range of 298 ± 10 K.

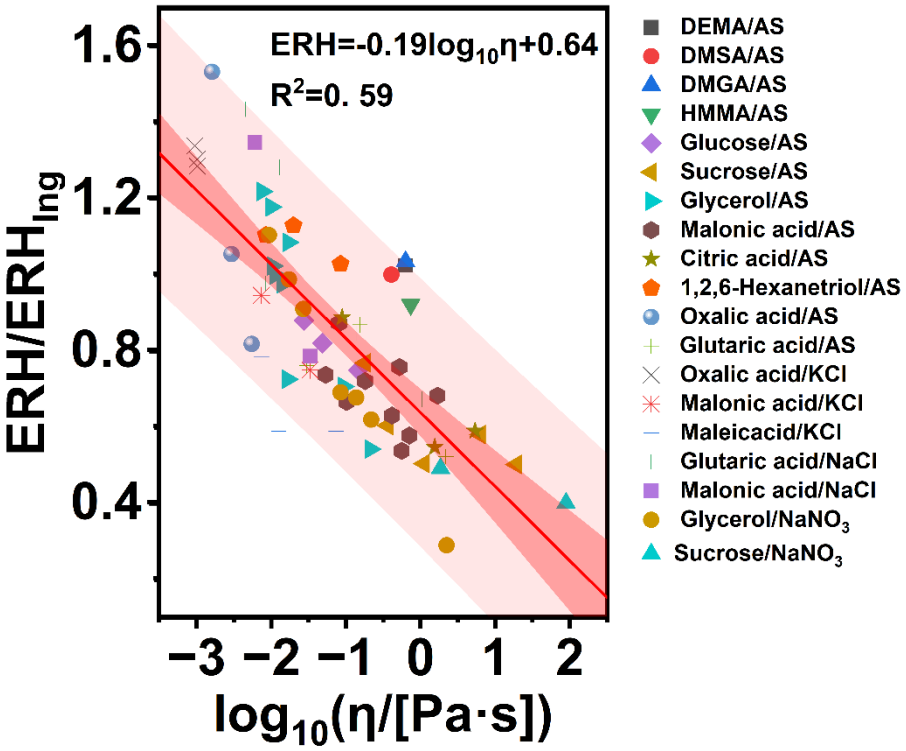

Figure S3. Linear fitting of aerosol normalized ERH for different organic-inorganic aerosols by using viscosity ($\log_{10}\eta$) as the predictor. The ERH of the organic-inorganic mixture systems was normalized according to ERHIng, which represents the ERH of the corresponding pure binary aqueous inorganic salt system at the same temperature (i.e., ERH/ERH_{Ing}. Data points are color- and shape-coded to distinguish between different organic and inorganic aerosol species. The red solid line represents the linear regression fit between viscosity and ERH. The dark pink band indicates the 95% confidence interval, while the light pink band shows the prediction interval. DEMA represents Diethyl malonic acid, DMSA represents 2,2-Dimethyl succinic acid, DMGA represents 3,3-Dimethyl glutaric acid, HMMA represents DL-4-Hydroxy-3-methoxymandelic acid and DHBA represents 2,5-Dihydroxybenzoic acid. All empirical ERH values were measured within a temperature range of 298 ± 10 K, and all viscosity values were calculated at 298 K.

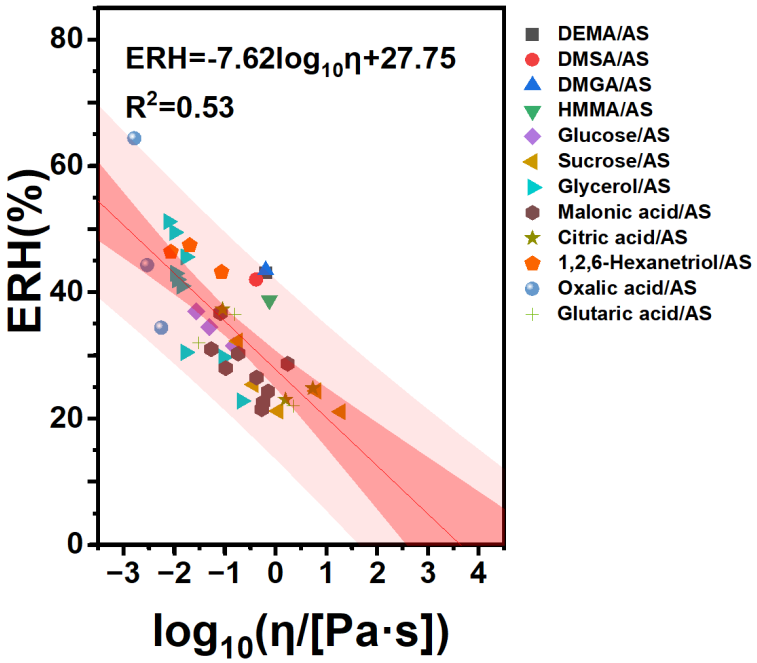

Figure S4. Linear fitting of aerosol ERH for different organic-ammonium sulfate aerosols by using viscosity ($\log_{10}\eta$) as the predictor. Data points are color- and shape-coded to distinguish between different organic and inorganic aerosol species. The red solid line represents the linear regression fit between viscosity and ERH. The dark pink band indicates the 95% confidence interval, while the light pink band shows the prediction interval. DEMA represents Diethyl malonic acid, DMSA represents 2,2-Dimethyl succinic acid, DMGA represents 3,3-Dimethyl glutaric acid, HMMA represents DL-4-Hydroxy-3-methoxymandelic acid and DHBA represents 2,5-Dihydroxybenzoic acid. All empirical ERH values were measured within a temperature range of 298 ± 10 K, and all viscosity values were calculated at 298 K.

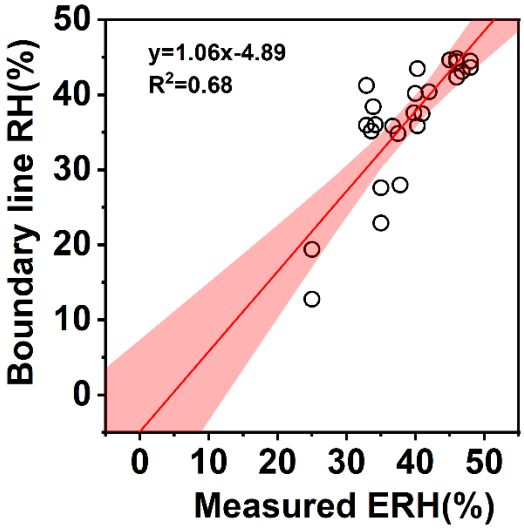

Figure S5. Comparison of measured ERH values versus model predicted ERH values based on the viscosity-ERH model by excluding the datapoints that are not effloresced (i.e., (0,0) data in Figure 3). The red line representing the linear regression fit to the data, along with the corresponding coefficient of determination (R^2). The fitted equation is y = 1.06x - 4.89, with slope close to unity and R^2 = 0.68. The pale pink shading represents the 95% confidence interval.

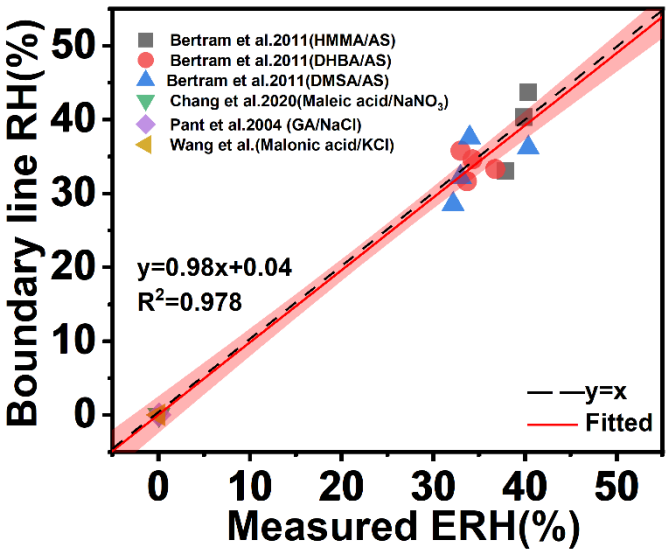

Figure S6. Comparison of measured ERH values versus model predicted ERH values based on the viscosity-T_g-ERH model. The black dashed line denotes the y=x, and the red line representing the linear regression fit to the data, along with the corresponding coefficient of determination (R^2), R^2=0.978. The pale pink shading represents the 95% confidence interval.

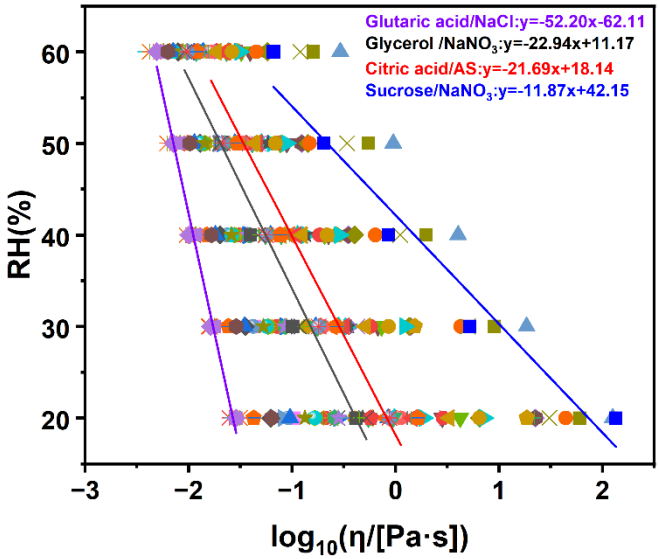

Figure S7. Relationship between relative humidity (RH) and aerosol viscosity for organic–inorganic mixed aerosol systems. Data points represent modeled viscosities for all aerosol systems listed in Table S1, including variations in both chemical composition and organic-to-inorganic mass ratio (OIR) over an RH range of 20% to 60%. Solid lines show linear fits for four representative systems: Glutaric acid/NaCl (OIR = 0.25, purple), Glycerol/$NaNO_3$ (OIR = 0.25, black), Citric acid/AS (OIR = 0.25, red), and Sucrose/$NaNO_3$ (OIR = 0.25, blue). Details of these representative systems are provided in Table S12. All viscosity values were calculated at 298 K.

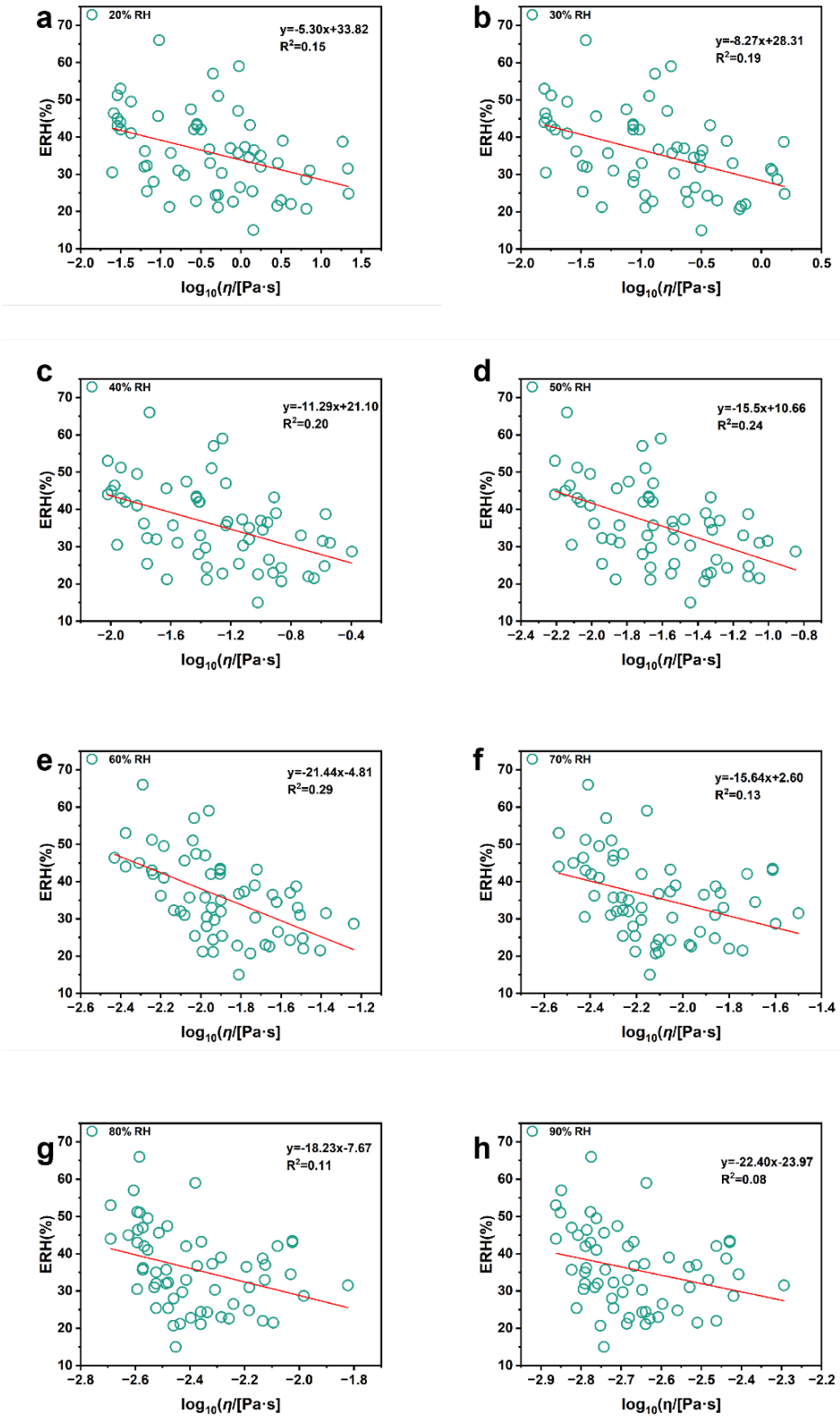

Figure S8. Relationships between ERH and aerosol viscosity calculated at fixed RH conditions. Panels (a–h) show ERH plotted against ($\log_{10}(\eta/[\mathrm{Pa\cdot s}])$), where η represents the aerosol viscosity calculated at fixed RH values of 20%, 30%, 40%, 50%, 60%, 70%, 80%, and 90%, respectively.All empirical ERH values were measured within a temperature range of 298 ± 10 K, and all viscosity values were calculated at 298 K.

References

Armeli, G., Peters, J.-H., and Koop, T.: Machine-Learning-Based Prediction of the Glass Transition Temperature of Organic Compounds Using Experimental Data, ACS Omega, 8, 12298–12309, https://doi.org/10.1021/acsomega.2c08146, 2023.

Armeli Iapichino, G., Peters, J.-H., and Koop, T.: Bielefeld Molecular Organic Glasses (BIMOG) Database, 2023.

Bertram, A. K., Martin, S. T., Hanna, S. J., Smith, M. L., Bodsworth, A., Chen, Q., Kuwata, M., Liu, A., You, Y., and Zorn, S. R.: Predicting the relative humidities of liquid-liquid phase separation, efflorescence, and deliquescence of mixed particles of ammonium sulfate, organic material, and water using the organic-to-sulfate mass ratio of the particle and the oxygen-to-carbon elemental ratio of the organic component, Atmospheric Chemistry and Physics, 11, 10995–11006, https://doi.org/10.5194/acp-11-10995-2011, 2011.

Braban, C. F. and Abbatt, J. P. D.: A study of the phase transition behavior of internally mixed ammonium sulfate - malonic acid aerosols, Atmospheric Chemistry and Physics, 4, 1451–1459, https://doi.org/10.5194/acp-4-1451-2004, 2004.

Cai, C., Luan, Y., Shi, X., and Zhang, Y.: $(NH_4)_2SO_4$ heterogeneous nucleation and glycerol evaporation of $(NH_4)_2SO_4$-glycerol system in its dynamic efflorescence process, Chemical Physics, 483–484, 140–148, https://doi.org/10.1016/j.chemphys.2016.12.003, 2017.

Chang, P.: Study on single aerosol particle by spontaneous and stimulated Raman spectroscopy. Ph.D. Dissertation, Beijing Institute of Technology, 2020.

Ghorai, S., Wang, B., Tivanski, A., and Laskin, A.: Hygroscopic properties of internally mixed particles composed of NaCl and water-soluble organic acids, Environ. Sci. Technol., 48, 2234–2241, https://doi.org/10.1021/es404727u, 2014.

Huang, Q., Pitta, K. R., Constantini, K., Ott, E.-J. E., Zuend, A., and Freedman, M. A.: Experimental phase diagram and its temporal evolution for submicron 2-methylglutaric acid and ammonium sulfate aerosol particles, Phys. Chem. Chem. Phys., 26, 2887–2894, https://doi.org/10.1039/D3CP04411D, 2024.

Ji, Z.-R., Zhang, Y., Pang, S.-F., and Zhang, Y.-H.: Crystal Nucleation and Crystal Growth and Mass Transfer in Internally Mixed Sucrose/NaNO3 Particles, J. Phys. Chem. A, 121, 7968–7975, https://doi.org/10.1021/acs.jpca.7b08004, 2017.

Laskina, O., Morris, H. S., Grandquist, J. R., Qin, Z., Stone, E. A., Tivanski, A. V., and Grassian, V. H.: Size matters in the water uptake and hygroscopic growth of atmospherically relevant multicomponent aerosol particles, J. Phys. Chem. A, 119, 4489–4497, https://doi.org/10.1021/jp510268p, 2015.

Li, Y., Day, D. A., Stark, H., Jimenez, J. L., and Shiraiwa, M.: Predictions of the glass transition temperature and viscosity of organic aerosols from volatility distributions, Atmospheric Chemistry and Physics, 20, 8103–8122, https://doi.org/10.5194/acp-20-8103-2020, 2020.

Ma, S., Chen, Z., Pang, S., and Zhang, Y.: Observations on hygroscopic growth and phase transitions of mixed 1, 2, 6-hexanetriol/$(NH_4)_2SO_4$ particles: investigation of the liquid–liquid phase separation (LLPS) dynamic process and mechanism and secondary LLPS during the dehumidification, Atmospheric Chemistry and Physics, 21, 9705–9717, https://doi.org/10.5194/acp-21-9705-2021, 2021.

Pant, A., Fok, A., Parsons, M. T., Mak, J., and Bertram, A. K.: Deliquescence and crystallization of

ammonium sulfate-glutaric acid and sodium chloride-glutaric acid particles, Geophysical Research Letters, 31, 2004GL020025, https://doi.org/10.1029/2004GL020025, 2004.

Parsons, M. T., Knopf, D. A., and Bertram, A. K.: Deliquescence and crystallization of ammonium sulfate particles internally mixed with water-soluble organic compounds, J. Phys. Chem. A, 108, 11600–11608, https://doi.org/10.1021/jp0462862, 2004.

Ren, H.-M., Cai, C., Leng, C.-B., Pang, S.-F., and Zhang, Y.-H.: Nucleation Kinetics in Mixed NaNO3/Glycerol Droplets Investigated with the FTIR–ATR Technique, J. Phys. Chem. B, 120, 2913–2920, https://doi.org/10.1021/acs.jpcb.5b12442, 2016.

Shi, X.-M., Wu, F.-M., Jing, B., Wang, N., Xu, L.-L., Pang, S.-F., and Zhang, Y.-H.: Hygroscopicity of internally mixed particles composed of (NH4)2SO4 and citric acid under pulsed RH change, Chemosphere, 188, 532–540, https://doi.org/10.1016/j.chemosphere.2017.09.024, 2017.

S. Sheldon, C., M. Choczynski, J., Morton, K., Diaz, T. P., D. Davis, R., and F. Davies, J.: Exploring the hygroscopicity, water diffusivity, and viscosity of organic–inorganic aerosols – a case study on internally-mixed citric acid and ammonium sulfate particles, Environmental Science: Atmospheres, 3, 24–34, https://doi.org/10.1039/D2EA00116K, 2023.

Ushijima, S. B., Huynh, E., Davis, R. D., and Tolbert, M. A.: Seeded crystal growth of internally mixed organic–inorganic aerosols: impact of organic phase state, J. Phys. Chem. A, 125, 8668–8679, https://doi.org/10.1021/acs.jpca.1c04471, 2021.

Wang, L.-N., Cai, C., and Zhang, Y.-H.: Kinetically Determined Hygroscopicity and Efflorescence of Sucrose-Ammonium Sulfate Aerosol Droplets under Lower Relative Humidity, J Phys Chem B, 121, 8551–8557, https://doi.org/10.1021/acs.jpcb.7b05551, 2017a.

Wang, X.: Study on the hygroscopicity of mixed aerosols composed of organic acids and inorganic salts by Raman spectroscopy.Ph.D. Dissertation, Beijing Institute of Technology, 2018.

Wang, X., Jing, B., Tan, F., Ma, J., Zhang, Y., and Ge, M.: Hygroscopic behavior and chemical composition evolution of internally mixed aerosols composed of oxalic acid and ammonium sulfate, Atmospheric Chemistry and Physics, 17, 12797–12812, https://doi.org/10.5194/acp-17-12797-2017, 2017b.

Wu, F.: Thermodynamics and Kinetics Research of Mixed Inorganic/Glutaric acid Aerosols in the Hygroscopic Process.Ph.D. Dissertation, Beijing Institute of Technology, 2017.

Xu, Y., Liu, P., Ma, S., Pei, W., Pang, S., and Zhang, Y.: Efflorescence kinetics of aerosols comprising internally-mixed ammonium sulfate and water-soluble organic compounds, Atmospheric Environment, 274, 119007, https://doi.org/10.1016/j.atmosenv.2022.119007, 2022.

Ye, Y., Sun, J., Fan, Y., Li, Y., Li, Q., He, C., Ma, S., Zhao, Z., and Xu, T.: Key Roles of Bulk Viscosity and Acidity on Liquid–Liquid Phase Separation of Atmospheric Organic–Inorganic Mixed Aerosols, J. Phys. Chem. A, 129, 3921–3930, https://doi.org/10.1021/acs.jpca.5c01182, 2025.

Yu, J.-Y., Zhang, Y., Zeng, G., Zheng, C.-M., Liu, Y., and Zhang, Y.-H.: Suppression of NaNO3 Crystal Nucleation by Glycerol: Micro-Raman Observation on the Efflorescence Process of Mixed Glycerol/$NaNO_3$/Water Droplets, J. Phys. Chem. B, 116, 1642–1650, https://doi.org/10.1021/jp210824e, 2012.